

High-order compact finite difference scheme for option pricing in stochastic volatility jump models

Bertram Düring^{a,*}, Alexander Pitkin^a

^a*Department of Mathematics, University of Sussex, Pevensey II, Brighton, BN1 9QH, United Kingdom.*

Abstract

We derive a new high-order compact finite difference scheme for option pricing in stochastic volatility jump models, e.g. in Bates model. In such models the option price is determined as the solution of a partial integro-differential equation. The scheme is fourth order accurate in space and second order accurate in time. Numerical experiments for the European option pricing problem are presented. We validate the stability of the scheme numerically and compare its efficiency and hedging performance to standard finite difference methods. The new scheme outperforms a standard discretisation based on a second-order central finite difference approximation in all our experiments. At the same time, it is very efficient, requiring only one initial LU -factorisation of a sparse matrix to perform the option price valuation. It can also be useful to upgrade existing implementations based on standard finite differences in a straightforward manner to obtain a highly efficient option pricing code.

Keywords: Option pricing, high-order compact finite differences, stochastic volatility jump model, Bates model

2010 MSC: 65M06, 91G20, 35Q91

1. Introduction

The classical model for pricing financial options is the model of Black and Scholes [3] who consider that the underlying follows a geometric Brownian motion with constant volatility. This allows for the derivation of simple, closed-form option price formulae, however it is unable to explain commonly observed features of option market prices, like the implied volatility smile (or smirk) and excess and random volatility. A wide range of option pricing models have been proposed in the literature to alleviate such shortcomings. Many of the most widely used models share one of the following two features: (i) introduction of further risk factors, very often stochastic volatility [23], most famously in the Heston stochastic volatility model [18]; (ii) jumps in the underlying stochastic processes, e.g. as already

*Corresponding author

Email addresses: bd80@sussex.ac.uk (Bertram Düring), A.H.Pitkin@sussex.ac.uk (Alexander Pitkin)

introduced by Merton [24]. In 1996, Bates [1] proposed to combine both features in one model, now commonly referred to as the Bates or Stochastic Volatility Jump (SVJ) model. In this model the option price is given as the solution of a partial integro-differential equation (PIDE), see e.g. [6]. It is able to capture the typical features of market option prices, allowing for improved flexibility introduced by stochastic volatility and at the same time being able to fit short-dated skews by the incorporation of jumps in the underlying's process. It now takes the position of a quasi market standard in option pricing applications.

For some option pricing models closed-form solutions are available for vanilla payoffs (see e.g. [7]) or at least approximate analytic expressions, see e.g. [2] and the literature cited therein. In general, however, one has to rely on numerical methods for pricing options.

For numerical methods for option pricing models with a single risk factor, leading to partial differential equations in one spatial dimension, e.g. variants of the the Black-Scholes model, there is a large mathematical literature, with many relying on standard finite difference methods (see e.g. [31] and the references therein). For one-dimensional models with jump-diffusion we refer to [6, 8, 4, 27, 28].

For option pricing models with more than one risk factor, e.g. in stochastic volatility models, which involve solving partial differential equations in two or more spatial dimensions, there are fewer works, e.g. [21] where different efficient methods for solving the American option pricing problem for the Heston model are proposed. Other approaches include finite element-finite volume [33], multigrid [5], sparse wavelet [20], FFT-based [26], spectral methods [32] and operator splitting techniques [19, 11, 14, 17, 12].

For problems which additionally include jumps in the underlying's process, and require the solution of PIDE in two or more spatial dimensions, there are even fewer works. We mention [29, 30] who propose an implicit-explicit time discretisation in combination with a standard, second-order finite difference discretisation in space and [15] who discuss and analyse an explicit discretisation.

More recently, high-order finite difference schemes (fourth order in space) have been proposed for the solving partial differential equations arising from stochastic volatility models. In [9] a high-order compact finite difference scheme for option pricing in the Heston model is derived. This approach is extended to non-uniform grids in [10], and to multiple space dimensions in [13].

The originality of the present work consists in proposing a new *implicit-explicit high-order compact finite difference scheme* for option pricing in Bates model, based on the approaches from [9] and [29]. We derive a new compact scheme that is fourth order accurate in space and second order accurate in time. We validate the stability of the scheme numerically and compare its efficiency and hedging performance to standard finite difference methods. The new scheme outperforms a standard discretisation based on a second-order central finite difference approximation in all our experiments. At the same time, it is very efficient, requiring only one initial *LU*-factorisation of a sparse matrix to perform the option price valuation. It can also be useful to upgrade existing implementations based on standard finite differences in a straightforward manner to obtain a highly efficient option pricing code.

This article is organised as follows. In the next section we recall Bates model for option

pricing and the related partial integro-differential equation. Section 3 is devoted to a variable transformation for the problem. The new scheme is derived in Section 4. The smoothing of the initial condition and the discretisation of the boundary conditions are discussed in Section 5. Results of our numerical experiments are shown Section 6. We present numerical convergence and stability results and investigate the efficiency of the scheme and its hedging performance. Section 7 concludes.

2. Bates Model

We recall the Bates model [1] which we focus our paper on. The Bates model is a stochastic volatility model which allows for jumps in returns. Within this model the behaviour of the asset value, S , and its variance, σ , is described by the coupled stochastic differential equations,

$$\begin{aligned} dS(t) &= \mu_B S(t)dt + \sqrt{\sigma(t)} S(t) dW_1(t) + S(t) dJ, \\ d\sigma(t) &= \kappa(\theta - \sigma(t)) + v\sqrt{\sigma(t)} dW_2(t), \end{aligned}$$

for $0 \leq t \leq T$ and with $S(0), \sigma(0) > 0$. Here, $\mu_B = r - \lambda\xi_B$ is the drift rate, where $r \geq 0$ is the risk-free interest rate. The jump process J is a compound Poisson process with intensity $\lambda \geq 0$ and $J+1$ has a log-normal distribution $p(\tilde{y})$ with the mean in $\log(\tilde{y})$ being γ and the variance in $\log(\tilde{y})$ being v^2 , i.e. the probability density function is given by

$$p(\tilde{y}) = \frac{1}{\sqrt{2\pi}\tilde{y}v} e^{-\frac{(\log \tilde{y} - \gamma)^2}{2v^2}}.$$

The parameter ξ_B is defined by $\xi_B = e^{\gamma + \frac{v^2}{2}} - 1$. The variance has mean level θ , κ is the rate of reversion back to mean level of σ and v is the volatility of the variance σ . The two Wiener processes W_1 and W_2 have correlation ρ .

By standard derivative pricing arguments for the Bates model, we obtain the partial integro-differential equation

$$\begin{aligned} \frac{\partial V}{\partial t} + \frac{1}{2} S^2 \sigma \frac{\partial^2 V}{\partial S^2} + \rho v \sigma S \frac{\partial^2 V}{\partial S \partial \sigma} + \frac{1}{2} v^2 \sigma \frac{\partial^2 V}{\partial \sigma^2} + (r - \lambda \xi_B) S \frac{\partial V}{\partial S} + \kappa(\theta - \sigma) \frac{\partial V}{\partial \sigma} - (r + \lambda) V \\ + \lambda \int_0^{+\infty} V(S\tilde{y}, v, t) p(\tilde{y}) d\tilde{y} = L_D V + L_I V, \quad (1) \end{aligned}$$

which has to be solved for $S, \sigma > 0$, $0 \leq t < T$ and subject to a suitable final condition, e.g. $V(S, \sigma, T) = \max(K - S, 0)$, in the case of a European put option, with K denoting the strike price. For clarity the operators $L_D V$ and $L_I V$ are defined as the differential part (including the term $-(r + \lambda)V$) and the integral part, respectively.

3. Transformation of the equation

Using the transformation of variables

$$x = \log S, \quad \tau = T - t, \quad y = \frac{\sigma}{v} \quad \text{and} \quad u = \exp(r + \lambda)V$$

we obtain

$$u_\tau = \frac{1}{2}vy \left(\frac{\partial^2 u}{\partial x^2} + \frac{\partial^2 u}{\partial y^2} \right) + \rho vy \frac{\partial^2 u}{\partial x \partial y} - \left(\frac{1}{2}vy - r + \lambda \xi_B \right) \frac{\partial u}{\partial x} + \kappa \frac{(\theta - vy)}{v} \frac{\partial u}{\partial y} + \exp(r + \lambda) L_I V, \quad (2)$$

which is now posed on $\mathbb{R} \times \mathbb{R}^+ \times (0, T)$, with

$$L_I V = \lambda \int_0^\infty V(S\tilde{y}, v, t) p(\tilde{y}) d\tilde{y}.$$

Applying the same transformation to the intergral term, L_I ,

$$\exp(r + \lambda) L_I V = \lambda \int_0^{+\infty} u(x\tilde{y}, y, \tau) p(\tilde{y}) d\tilde{y}.$$

Now by setting $z = \log \tilde{y}$, $\tilde{u}(z, y, \tau) = u(e^z, y, \tau)$ and $\tilde{p}(z) = e^z p(e^z)$ we have

$$\exp(r + \lambda) L_I V = \lambda \int_0^{+\infty} u(x\tilde{y}, y, \tau) p(\tilde{y}) d\tilde{y} = \lambda \int_{-\infty}^{+\infty} \tilde{u}(x + z, y, \tau) \tilde{p}(z) dz.$$

The problem is completed by the following initial and boundary conditions:

$$\begin{aligned} u(x, y, 0) &= \max(1 - \exp(x), 0), \quad x \in \mathbb{R}, y > 0, \\ u(x, y, t) &\rightarrow 1, \quad x \rightarrow -\infty, y > 0, t > 0, \\ u(x, y, t) &\rightarrow 0, \quad x \rightarrow +\infty, y > 0, t > 0, \\ u_y(x, y, t) &\rightarrow 0, \quad x \in \mathbb{R}, y \rightarrow \infty, t > 0, \\ u_y(x, y, t) &\rightarrow 0, \quad x \in \mathbb{R}, y \rightarrow 0, t > 0. \end{aligned}$$

4. Implicit-explicit scheme

Following the idea employed by Salmi, Toivanen and von Sydow in [29, 30], we accomplish the implicit-explicit discretisation in time by means of the IMEX-CN method. This method is an adaptation of the Crank-Nicholson method, whereby an explicit treatment is added for the integral operator. To achieve high-order convergence we utilise the high-order compact finite difference scheme developed in [9] to implicitly approximate the differential operator, while we evaluate the integral explicitly using the Simpson's rule to match the high-order accuracy of the high-order compact scheme.

4.1. High-order compact scheme for the differential operator

Following the discretisation employed in [9], we replace \mathbb{R} by $[-R_1, R_1]$ and \mathbb{R}^+ by $[L_2, R_2]$ with $R_1, R_2 > L_2 > 0$. We consider a uniform grid $Z = \{x_i \in [-R_1, R_1] : x_i = ih_1, i = -N, \dots, N\} \times \{\sigma_j \in [L_2, R_2] : \sigma_j = L_2 + jh_2, j = 0, \dots, M\}$ consisting of $(2N + 1) \times (M + 1)$ grid points with $R_1 = Nh_1$, $R_2 = L_2 + Mh_2$ and with space steps h_1, h_2 and time step k . Let $u_{i,j}^n$ denote the approximate solution of (2) in (x_i, σ_j) at the time $t_n = nk$ and let $u^n = (u_{i,j}^n)$.

4.1.1. Elliptic problem

We introduce the high-order compact discretisation for the elliptic problem with Laplacian operator,

$$-\frac{1}{2}vy\left(\frac{\partial^2 u}{\partial x^2} + \frac{\partial^2 u}{\partial y^2}\right) - y\rho v\frac{\partial^2 u}{\partial x\partial y} - \left(r - \frac{1}{2}vy - \lambda\xi_B\right)\frac{\partial u}{\partial x} - \kappa\frac{(\theta - vy)}{v}\frac{\partial u}{\partial y} = f(x, y). \quad (3)$$

We construct a fourth-order compact finite difference scheme with a nine-point computational stencil using the eight nearest neighbouring points around a reference grid point (i, j) , following the approach in [9]. The idea behind the derivation of the high-order compact scheme is to operate on the differential equations as an auxiliary relation to obtain finite difference approximations for high-order derivatives in the truncation error. Inclusion of these expressions in a central difference approximation increases the order of accuracy while retaining a compact computational stencil.

Introducing a uniform grid with mesh spacing $h = h_1 = h_2$ in both the x - and y -directions, the standard central difference approximation to equation (3) at grid point (i, j) is

$$-\frac{1}{2}vy_j(\delta_x^2 u_{i,j} + \delta_y^2 u_{i,j}) - \rho vy_j \delta_x \delta_y u_{i,j} + \left(\frac{1}{2}vy_j - r + \lambda\xi_B\right)\delta_x u_{i,j} - \kappa\frac{(\theta - vy_j)}{v}\delta_y u_{i,j} - \tau_{i,j} = f(i, j), \quad (4)$$

where δ_x and δ_x^2 (δ_y and δ_y^2 , respectively) denote the first and second order central difference approximations with respect to x (with respect to y). The associated truncation error is given by

$$\tau_{i,j} = \frac{1}{24}vyh^2(u_{xxxx} + u_{yyyy}) + \frac{1}{6}\rho vyh^2(u_{xyyy} + u_{xxxy}) + \frac{1}{12}(2r - vy - 2\lambda\xi_B)h^2u_{xxx} + \frac{1}{6}\frac{\kappa(\theta - vy)}{v}h^2u_{yyy} + \mathcal{O}(h^4). \quad (5)$$

For the sake of clarity the subindices j and (i, j) on y_j and $u_{i,j}$ (and its derivatives) are omitted from here. Differentiating (3) with respect to x and y , respectively, yields,

$$u_{xxx} = -u_{xyy} - 2\rho u_{xyx} + \frac{2\lambda\xi_B + vy - 2r}{vy}u_{xx} - \frac{2\kappa(-vy + \theta)}{yv^2}u_{xy} - \frac{2}{vy}f_x, \quad (6)$$

$$u_{yyy} = -u_{yxx} - 2\rho u_{yyx} - \frac{1}{y}u_{xx} + \frac{2\lambda\xi_B - 2\rho v + vy - 2r}{vy}u_{yx} - \frac{-2\kappa vy + 2\kappa\theta + v^2}{v^2y}u_{yy} + \frac{1}{y}u_x + \frac{2\kappa}{vy}u_y - \frac{2}{vy}f_y. \quad (7)$$

Differentiating equations (6) and (7) with respect to y and x , respectively, and adding the

two expressions we obtain

$$u_{xyyy} + u_{xxxy} = -2\rho u_{xxyy} - \frac{u_{xxx}}{2y} + \frac{(2\lambda\xi_B - \rho v + vy - 2r)u_{xxy}}{vy} - \frac{(-4\kappa vy + 4\kappa\theta + v^2)u_{xyy}}{2yv^2} - \frac{(2\lambda\xi_B - vy - 2r)u_{xx}}{2vy^2} + \frac{\kappa(vy + \theta)u_{xy}}{y^2v^2} + \frac{f_x}{vy^2}. \quad (8)$$

By differentiating equation (3) twice with respect to x and twice with respect to y and adding the two expressions, we obtain

$$u_{xxxx} + u_{yyyy} = -2\rho u_{xxxy} - 2\rho u_{xyyy} - 2u_{xxyy} + 2\frac{(\kappa vy - v^2 - \kappa\theta)}{v^2y}u_{xxy} - \frac{(2r - vy - 2\lambda\xi_B)}{vy}u_{xxx} + 2\frac{(\kappa vy - v^2 - \kappa\theta)}{v^2y}u_{yyy} - \frac{(-vy + 4\rho v - 2\lambda\xi_B + 2r)}{vy}u_{xyy} + 4\frac{\kappa}{vy}u_{yy} + \frac{2}{y}u_{xy} - \frac{2}{vy}(f_{xx} + f_{yy}). \quad (9)$$

We now substitute equations (6)–(9) into (5) to yield a new expression of the error term $\tau_{i,j}$ that only consists of terms which are either $\mathcal{O}(h^4)$ or $\mathcal{O}(h^2)$ multiplied by derivatives of u which can be approximated to $\mathcal{O}(h^2)$ within the compact stencil. Inserting this new expression for the error term in (4) we obtain the following $\mathcal{O}(h^4)$ approximation to the partial differential equation (3),

$$\begin{aligned} & -\frac{1}{24} \frac{4h^2\lambda\xi_B(\lambda\xi_B + \rho v - 2) + vy_j(vy_j - 2\kappa - 2r) - 2(r\rho v + \kappa\theta + 2r^2 - v^2) + 12v^2y_j^2}{vy_j} \delta_x^2 u_{i,j} \\ & -\frac{1}{12} \frac{2h^2\kappa^2v^2y_j^2 - 4h^2\kappa^2\theta vy_j - h^2\kappa v^3y_j + 2h^2\kappa^2\theta^2 - h^2\kappa\theta v^2 - h^2v^4 + 6v^4y_j^2}{v^3y_j} \delta_y^2 u_{i,j} \\ & -\frac{1}{12} vy_j h^2 (2\rho^2 + 1) \delta_x^2 \delta_y^2 u_{i,j} - \frac{1}{6} \frac{(-2v\lambda\rho\xi_B - y_j\rho v^2 - \kappa vy_j + 2vr\rho + \kappa\theta)h^2}{v} \delta_x^2 \delta_y u_{i,j} \\ & -\frac{1}{12} \frac{(-4\kappa\rho vy_j + 4\rho\kappa\theta - 2\lambda v\xi_B - y_jv^2 + 2rv)h^2}{v} \delta_x \delta_y^2 u_{i,j} \\ & + \frac{1}{6} \frac{h^2\kappa(\rho v^2y_j + v^2y_j^2 - 2rvy_j - \theta vy_j + 2vy_j\xi_B + 2r\theta - 2\theta\xi_B) - h^2v^2(\rho v - r + \xi_B)}{v^2y_j} \delta_x \delta_y u_{i,j} \\ & + \frac{1}{12} \frac{-h^2\kappa y_j v + h^2\kappa\theta - h^2v^2 + 12vy_j\lambda\xi_B + 6y_j^2v^2 - 12vy_jr}{vy_j} \delta_x u_{i,j} \\ & + \frac{1}{6} \frac{\kappa(-h^2\kappa y_j v + h^2\kappa\theta - h^2v^2 + 6y_j^2v^2 - 6\theta vy_j)}{v^2y_j} \delta_y u_{i,j} \\ & = f_{i,j} + \frac{h^2}{6} \frac{\rho}{v} \delta_x \delta_y f_{i,j} - \frac{h^2}{6} \frac{(v^2 + \kappa(vy_j - \theta))}{v^2y_j} \delta_y f_{i,j} - \frac{h^2}{12} \frac{(2\lambda\xi_B + 2\rho v + vy_j - 2r)}{vy_j} \delta_x f_{i,j} \\ & \quad + \frac{h^2}{12} \delta_x^2 f_{i,j} + \frac{h^2}{12} \delta_y^2 f_{i,j} \quad (10) \end{aligned}$$

The fourth-order compact scheme (10) considered at mesh point (i, j) involves the nearest eight neighbouring meshpoints. Associated to the shape of the computational stencil, we

introduce indexes for each node from zero to eight,

$$\begin{pmatrix} u_{i-1,j+1} = u_6 & u_{i,j+1} = u_2 & u_{i+1,j+1} = u_5 \\ u_{i-1,j} = u_3 & u_{i,j} = u_0 & u_{i+1,j} = u_1 \\ u_{i-1,j-1} = u_7 & u_{i,j-1} = u_4 & u_{i+1,j-1} = u_8 \end{pmatrix}.$$

With this indexing the scheme (10) is defined by

$$\sum_{l=0}^8 \alpha_l u_l = \sum_{l=0}^8 \gamma_l f_l,$$

with the coefficients α_l and γ_l given by

$$\begin{aligned} \alpha_0 &= \left(\frac{4\kappa^2 + v^2}{12v} - \frac{v(2\rho^2 - 5)}{3h^2} \right) y - \frac{2\kappa^2\theta + \kappa v^2 + rv^2 - v^2\xi_B}{3v^2} \\ &\quad + \frac{-r\rho v^3 + \rho v^3\xi_B + \kappa^2\theta^2 + r^2v^2 - 2rv^2\xi_B - v^4 + v^2\xi_B^2}{3v^3y}, \\ \alpha_{1,3} &= \left(-\frac{v}{24} + \frac{2\kappa\rho \pm v}{6h} + \frac{v(\rho-1)(\rho+1)}{3h^2} \right) y \mp \frac{1}{24}\kappa h + \frac{\kappa}{12} + \frac{r}{6} - \frac{\xi_B}{6} \pm \frac{\kappa\rho\theta - rv + v\xi_B}{3vh} \\ &\quad + \frac{1}{y} \left(\pm \frac{(\kappa\theta - v^2)h}{24v} - \frac{-2r\rho v + 2\rho v\xi_B + \kappa\theta + 2r^2 - 4r\xi_B - v^2 + 2\xi_B^2}{12v} \right), \\ \alpha_{2,4} &= \left(\frac{\kappa^2}{6v} + \frac{\mp\rho v \pm 2\kappa}{6h} + \frac{v(\rho-1)(\rho+1)}{3h^2} \right) y \mp \frac{\kappa^2 h}{12v} + \frac{\kappa(4\kappa\theta + v^2)}{12v^2} - \frac{-r\rho v + \rho v\xi_B + \kappa\theta}{3vh} \\ &\quad + \frac{1}{y} \left(\frac{\kappa(\kappa\theta - v^2)h}{12v^2} - \frac{(2\kappa\theta + v^2)(\kappa\theta - v^2)}{12v^3} \right), \\ \alpha_{5,7} &= \left(-\frac{\kappa}{24} \pm \frac{(2\rho+1)(2\kappa+v)}{24h} - \frac{v(\rho+1)(2\rho+1)}{12h^2} \right) y + \frac{\kappa(\rho v + 2r + \theta - 2\xi_B)}{24v} \\ &\quad \mp \frac{(2\rho+1)(\kappa\theta + rv - v\xi_B)}{12vh} - \frac{-\rho v^3 + 2\kappa r\theta - 2\kappa\theta\xi_B - rv^2 + v^2\xi_B}{24v^2y}, \\ \alpha_{6,8} &= \left(\frac{\kappa}{24} \mp \frac{(2\rho-1)(2\kappa-v)}{24h} - \frac{v(2\rho-1)(\rho-1)}{12h^2} \right) y - \frac{\kappa(\rho v + 2r + \theta - 2\xi_B)}{24v} \\ &\quad \pm \frac{(2\rho-1)(\kappa\theta - rv + v\xi_B)}{12vh} + \frac{-\rho v^3 + 2\kappa r\theta - 2\kappa\theta\xi_B - rv^2 + v^2\xi_B}{24v^2y}, \end{aligned}$$

and

$$\begin{aligned} \gamma_0 &= 2/3, \quad \gamma_{1,3} = \frac{1}{12} \mp \frac{h}{24} \pm \frac{(-\rho v + r - \xi_B)h}{12vy}, \quad \gamma_{2,4} = \frac{1}{12} \mp \frac{\kappa h}{12v} \pm \frac{(\kappa\theta - v^2)h}{12v^2y}, \\ \gamma_5 &= \gamma_7 = \frac{\rho}{24}, \quad \gamma_6 = \gamma_8 = -\frac{\rho}{24}. \end{aligned}$$

When multiple indexes are used with \pm and \mp signs, the first index corresponds to the upper sign.

4.1.2. Extension to the parabolic problem

To extend the above approach to the parabolic problem we replace $f(x, y)$ with the time derivative. We consider the class of two time step methods. By differencing at $t_\mu = (1 - \mu)t_n + \mu t^{n+1}$, where $0 \leq \mu \leq 1$ and the superscript n denotes the time level, we yield a set of integrators including the forward and backward Euler scheme, ($\mu = 0$) and ($\mu = 1$), respectively, and the Crank-Nicolson scheme ($\mu = 1/2$). By defining $\delta_t^+ u^n = \frac{u^{n+1} - u^n}{k}$, the resulting fully discrete difference scheme of node (i, j) at the time level n becomes

$$\sum_{l=0}^8 \mu \alpha_l u_l^{n+1} + (1 - \mu) \alpha_l u_l^n = \sum_{l=0}^8 \gamma_l \delta_t^+ u_l^n,$$

which can be written as

$$\sum_{l=0}^8 \beta_l u_l^{n+1} = \sum_{l=0}^8 \zeta_l u_l^n.$$

with the coefficients β_l and ζ_l given by

$$\begin{aligned} \beta_0 &= (((2y_j^2 - 8)v^4 + ((-8\kappa - 8r + 8\xi_B)y_j - (8r + 8\xi_B)\rho)v^3 + (8\kappa^2 y_j^2 + 8r^2 - 16r\xi_B + 8\xi_B)v^2 \\ &\quad - 16\kappa^2 \theta v y_j + 8\kappa^2 \theta^2) \mu k + 16v^3 y_j) h^2 + (16\rho^2 + 40) y_j^2 v^4 \mu k \\ \beta_{1,3} &= \pm ((\kappa \theta v^2 - v^4 - \kappa y_j v^3) \mu k - (y_j + 2\rho) v^3 + 2v^2 r - 2v^2 \xi_B) h^3 + (((-y_j^2 + 2)v^4 \\ &\quad + ((4r - 4\xi_B + 2\kappa)y_j + 4\rho r - 4\rho \xi_B) v^3 - (2\kappa \theta + 4r^2 - 4x_B^2 + 8r\xi_B) v^2) \mu k + 2v^3 y_j) h^2 \\ &\quad \pm (4v^4 y_j^2 + (-8y_j^2 \kappa \rho - 8y_j r + 8y_j \xi_B) v^3 + 8y_j \kappa \theta \rho v^2) \mu k h + (8\rho^2 - 8) y_j^2 v^4 \mu k, \\ \beta_{2,4} &= \pm ((2\kappa^2 \theta v - 2\kappa^2 v^2 y_j - 2v^3 \kappa) \mu k - 2v^2 y_j \kappa + 2v \kappa \theta - 2v^3) h^3 + ((2v^4 + 2\kappa y_j v^3 \\ &\quad + (-4\kappa^2 y_j^2 + 2\kappa \theta) v^2 + 8\kappa^2 v y_j - 4\kappa^2 \theta^2) \mu k + 2v^3 y_j) h^2 \pm ((8y_j^2 \kappa + 8y_j \rho r - 8y_j \rho \xi_B) v^3 \\ &\quad - 4v^4 y_j^2 \rho - 8v^2 y_j \kappa \theta) \mu k h + (8\rho^2 - 8) y_j^2 v^4 \mu k, \\ \beta_{5,7} &= ((v^4 \rho + (-y^2 \kappa + \kappa y_j \rho + r - \xi_B) v^3 + (\theta + 2r - 2\xi_B) \kappa y_j v^2 - 2r \kappa \theta v + 2\xi_B \kappa \theta v) \mu k + v^3 \rho y_j) h^2 \\ &\quad \pm ((2\rho + 1) y_j^2 v^4 + ((2 + 4\rho) \kappa y_j^2 + (-2r + 2\xi_B - 4\rho r + 4\rho \xi_B) y_j) v^3 + (-4\theta \rho - 2\theta) \kappa y_j v^2) \mu k h \\ &\quad + (-4\rho^2 - 6\rho - 2) y_j^2 v^4 \mu k, \\ \beta_{6,8} &= ((-v^4 \rho + (y^2 \kappa - \kappa y_j \rho - r + \xi_B) v^3 + (-\theta - 2r + 2\xi_B) \kappa y_j v^2 + 2r \kappa \theta v - 2\xi_B \kappa \theta v) \mu k - v^3 \rho y_j) h^2 \\ &\quad \pm ((2\rho - 1) y_j^2 v^4 + ((2 - 4\rho) \kappa y_j^2 + (2r - 2\xi_B - 4\rho r + 4\rho \xi_B) y_j) v^3 + (4\theta \rho - 2\theta) \kappa y_j v^2) \mu k h \\ &\quad + (-4\rho^2 + 6\rho - 2) y_j^2 v^4 \mu k, \end{aligned}$$

and

$$\begin{aligned} \zeta_0 &= 16v^3 y_j h^2 + (1 - \mu) k (((8 - 2y_j^2) v^4 + ((8\kappa + 8r - 8\xi_B) y_j + 8\rho r - 8\rho \xi_B) v^3 \\ &\quad + (-8r^2 - 8\xi_B^2 + 16r\xi_B - 8\kappa^2 y_j^2) v^2 + 16\kappa^2 \theta v y_j - 8\kappa^2 \theta^2) h^2 + (-40 + 16\rho^2) y_j^2 v^4), \\ \zeta_{1,3} &= \pm (2r - 2\xi_B - (y_j + 2\rho) v) v^2 h^3 + 2v^3 y_j h^2 + (1 - \mu) k (\pm (v \kappa y_j + v^2 - \kappa \theta) v^2 h^3 \\ &\quad + (v^2 y_j^2 - (4r + 4\xi_B + 2\kappa) v y_j + 4r^2 + 4\xi_B^2 + 2\kappa \theta + 2v y_j - 4\rho v r + 4\rho v \xi_B) v^2 h^2 \\ &\quad \pm ((-4v + 8\kappa \rho) v^3 y_j^2 + (-8\kappa \theta \rho + 8v r - 8v \xi_B) v^2 y_j) h + (8v^2 - 8v^2 \rho^2) v^2 y_j^2), \end{aligned}$$

$$\begin{aligned}
\zeta_{2,4} &= \pm (2v\kappa\theta - 2v^2y_j\kappa - 2v^3)h^3 + 2v^3y_jh^2 + (1-\mu)k(\pm(v\kappa y_j + v^2 - \kappa\theta)v^2h^3 \\
&\quad + (v^2y_j^2 - (4r + 2\kappa)vy_j + 2\kappa\theta(2\kappa\theta - v^2) - 2v^4)h^2 \pm ((-8v^3\kappa + 4v^4\rho)y_j^2 \\
&\quad + (8\kappa\theta v^2 - 8v^3\rho r)y_j)h + (-8v^4\rho^2 + 8v^4)y_j^2), \\
\zeta_{5,7} &= v^3\rho y_jh^2 + (1-\mu)k((v^3y_j^2\kappa - v(v\kappa\theta + 2r\kappa v - 2\xi_B\kappa v + \kappa v^2\rho)y_j) \\
&\quad - v(v^2r - 2v^2\xi_B - 2r\kappa\theta + 2\xi_B\kappa\theta + v^3\rho))h^2 \pm (-v(2v^3\rho + v^3 + 4\kappa v^2\rho + 2v^2\kappa)y_j^2 \\
&\quad + v(2v\kappa\theta + 4v\kappa\theta\rho + 4v^2\rho r + 4v^2\rho\xi_B + 2v^2r + 2v^2\xi_B)y_j)h + v(2v^3 + 6v^3\rho + 4v^3\rho^2)y_j^2), \\
\zeta_{6,8} &= -v^3\rho y_jh^2 + (1-\mu)k((-v^3y_j^2\kappa + v(v\kappa\theta + 2r\kappa v - 2\xi_B\kappa v + \kappa v^2\rho)y_j \\
&\quad + v(v^2r - v^2\xi_B - 2r\kappa\theta + 2\xi_B\kappa\theta + v^3\rho)) \pm (v(-2v^3\rho + v^3 + 4\kappa v^2\rho - 2v^2\kappa)y_j^2 \\
&\quad + v(2v\kappa\theta - 4v\kappa\theta\rho + 4v^2\rho r - 4v^2\rho\xi_B - 2v^2r - 2v^2\xi_B)y_j)h + v(2v^3 - 6v^3\rho + 4v^3\rho^2)y_j^2).
\end{aligned}$$

Where multiple indexes are used with \pm and \mp signs, the first index corresponds to the upper sign. The Crank-Nicholson scheme is used by setting $\mu = 1/2$, yielding a scheme which is second-order accurate in time and fourth-order accurate in space.

4.2. Integral operator

After the initial transformation of variables we have the integral operator in the following form,

$$L_I = \lambda \int_{-\infty}^{+\infty} \tilde{u}(x+z, y, \tau) \tilde{p}(z) dz,$$

where the probability density function, $\tilde{p}(z)$ is given by

$$\tilde{p}(z) = \frac{1}{\sqrt{2\pi}zv} e^{-\frac{(\log(z) - \gamma)^2}{2v^2}}.$$

We make a final change of variables $\zeta = x + z$ with the intention of studying the value of the integral at the point x_i ,

$$\begin{aligned}
I_i &= \int_{-\infty}^{+\infty} \tilde{u}(\zeta, y, \tau) \tilde{p}(\zeta - x_i) d\zeta = \int_{x_{min}}^{x_{max}} \tilde{u}(\zeta, y, \tau) \tilde{p}(\zeta - x_i) d\zeta + \int_{x_{max}}^{\infty} \tilde{u}(\zeta, y, \tau) \tilde{p}(\zeta - x_i) d\zeta \\
&\quad + \int_{-\infty}^{x_{min}} \tilde{u}(\zeta, y, \tau) \tilde{p}(\zeta - x_i) d\zeta. \quad (11)
\end{aligned}$$

4.2.1. Simpson's rule

To estimate the integral we require a numerical integration method of high order to match our finite difference scheme, we choose to use the composite Simpson's rule, defined as

$$\int_a^b f(x)dx \approx \frac{h}{3} \left[f(x_0) + 2 \sum_{j=1}^{n/2-1} f(x_{2j}) + 4 \sum_{j=1}^{n/2} f(x_{2j-1}) + f(x_n) \right].$$

The error committed by the composite Simpson's rule is bounded by

$$\frac{h^4}{180} (b-a) \max_{\xi \in [a,b]} |f^{(4)}(\xi)|.$$

Through the choice of the interval (x_{min}, x_{max}) we can assure that the integrals outside this range are of negligible value. Allowing the integral to be evaluated using Simpsons rule on a equidistant grid in x with spacing Δx and m_x grid-points in (x_{min}, x_{max}) , where each interval has length mesh-size $h/2$. Equation (11) can now be written as,

$$I_i \approx \int_{x_{min}}^{x_{max}} \tilde{u}(\zeta, y, \tau) \tilde{p}(\zeta - x_i) d\zeta$$

$$\approx \frac{\Delta x}{3} \sum_{j=1}^{\frac{m_x}{2}} [\tilde{u}(\zeta_{2j-2}, y, \tau) \tilde{p}(\zeta_{2j-2} - x_i) + 4\tilde{u}(\zeta_{2j-1}, y, \tau) \tilde{p}(\zeta_{2j-1} - x_i)$$

$$+ \tilde{u}(\zeta_{2j}, y, \tau) \tilde{p}(\zeta_{2j} - x_i)] = \tilde{I}_i. \quad (12)$$

This computation is calculated explicitly at each time-step by the matrix-vector equation, $\tilde{I} = W_{m_x} \tilde{u}$, defined as follows,

$$\tilde{I} = \begin{pmatrix} \tilde{I}_1 & \tilde{I}_3 & \dots & \tilde{I}_{m_x-1/2} & \tilde{I}_{m_x/2} \end{pmatrix}^\top, \quad \tilde{u} = (\tilde{u}_1 \quad \tilde{u}_3 \quad \dots \quad \tilde{u}_{m_x-1/2} \quad \tilde{u}_{m_x/2})^\top,$$

$$W_{m_x} = \begin{bmatrix} \tilde{p}(\zeta_0 - x_0) & 4\tilde{p}(\zeta_1 - x_0) & 2\tilde{p}(\zeta_2 - x_0) & \dots & \tilde{p}(\zeta_{m_x} - x_0) \\ \tilde{p}(\zeta_0 - x_1) & 4\tilde{p}(\zeta_1 - x_1) & 2\tilde{p}(\zeta_2 - x_1) & \dots & \tilde{p}(\zeta_{m_x} - x_1) \\ \vdots & \vdots & \vdots & \ddots & \vdots \\ \tilde{p}(\zeta_0 - x_{m_x}) & 4\tilde{p}(\zeta_1 - x_{m_x}) & 2\tilde{p}(\zeta_2 - x_{m_x}) & \dots & \tilde{p}(\zeta_{m_x} - x_{m_x}) \end{bmatrix}.$$

The integral operator, L_I , is estimated over (x_{min}, x_{max}) using Simpson's rule. The tails could be discarded as they are assumed to be of negligible value for sufficiently small (large) choice of x_{min} (x_{max}). A direct result of this approach would be the necessity to compute the option price over a wider domain than practically relevant. To alleviate this issue we assume that the option price follows the payoff function outside of the range (x_{min}, x_{max}) , and approximate the tails by the following integrals

$$\int_{x_{max}}^{\infty} \tilde{u}(\zeta, y, \tau) \tilde{p}(\zeta) d\zeta \approx \int_{x_{max}}^{\infty} \max(1 - \exp(\zeta), 0) \tilde{p}(\zeta) d\zeta,$$

$$\int_{-\infty}^{x_{min}} \tilde{u}(\zeta, y, \tau) \tilde{p}(\zeta) d\zeta \approx \int_{-\infty}^{x_{min}} \max(1 - \exp(\zeta), 0) \tilde{p}(\zeta) d\zeta.$$

The value of the first of these integrals is trivial as the payoff function is zero in the region $(x_{max}, +\infty)$. We estimate the second integral using Simpson's rule on an equal-sized adjacent equidistant grid to our original grid.

4.3. Time discretisation for IMEX method

Having set the framework for the discretisation of the operators L_D and L_I , we now introduce the implicit-explicit method,

$$\sum_{l=0}^8 \beta_l u^{n+1} = \sum_{l=0}^8 \zeta_l \left(1 + \frac{3\Delta\tau}{2} L_I \right) u^n - \sum_{l=0}^8 \zeta_l \left(\frac{\Delta\tau}{2} L_I \right) u^{n-1}.$$

5. Initial condition and boundary conditions

5.1. Initial condition

The initial condition is given by the transformed payoff function of the put option,

$$u(x, \sigma, 0) = \max(1 - \exp(x), 0), \quad x \in \mathbb{R}, \sigma > 0.$$

To maintain the order of the scheme we smooth this function around the singular point, this follows from [22] which states that we cannot expect to achieve fourth order convergence if the initial condition is not sufficiently smooth. In [22] suitable smoothing operators are defined in the Fourier space. Since the order of convergence of our high-order compact scheme is four we follow [13] and select the smoothing operator ϕ_4 , given by its Fourier transform

$$\phi_4(\omega) = \left(\frac{\sin(\omega/2)}{\omega/2} \right)^4 \left[1 + \frac{2}{3} \sin^2(\omega/2) \right].$$

This leads to the smoothed initial condition

$$\tilde{u}_0(x_1, x_2) = \frac{1}{h^2} \int_{-3h}^{3h} \int_{-3h}^{3h} \phi_4\left(\frac{x}{h}\right) \phi_4\left(\frac{y}{h}\right) u_0(x_1 - x, x_2 - y) dx dy.$$

As $h \rightarrow 0$, this smoothed initial condition converges to the original initial condition. The results in [22] prove high-order convergence of the approximation to the smoothed problem to the true solution of (2).

Note that in [9] a Rannacher style smoothing start-up [25] is used with four fully implicit quarter time steps. In our experiments we notice no benefit by employing such a start-up, and use the Crank-Nicolson time stepping throughout. Since the coefficients in (2) do not depend on time, we are required to build up the discretisation matrices for the new scheme only once. They can then be *LU*-factorised once, and the factorisation can be used in each time step, leading to a highly efficient scheme.

5.2. Boundary conditions

We impose artificial boundary conditions as follows. Due to the compactness of the scheme, the Dirichlet boundary conditions are considered without introduction of numerical error by imposing

$$u_{-N,j}^n = 1 - e^{rt_n - Nh}, \quad u_{+N,j}^n = 0, \quad j = 0, \dots, M.$$

At the other boundaries we impose homogeneous Neumann boundary conditions, these require more attention as no value is prescribed, therefore, they must be set by extrapolation from values in the interior. Here the introduction of numerical error must be negated by choice of an extrapolation formulae of order high enough not to affect the overall order of accuracy. We choose the following extrapolation formulae:

$$\begin{aligned} u_{i,0}^n &= 4u_{i,1}^n - 6u_{i,2}^n + 4u_{i,3}^n - u_{i,4}^n + \mathcal{O}(h^4), \quad i = -N+1, \dots, N-1, \\ u_{i,M}^n &= 4u_{i,M-1}^n - 6u_{i,M-2}^n + 4u_{i,M-3}^n - u_{i,M-4}^n + \mathcal{O}(h^4), \quad i = -N+1, \dots, N-1. \end{aligned}$$

6. Numerical Experiments

We implement the algorithm using C++ and conduct a number of numerical experiments to assess the convergence and stability of the scheme. Below we present Figure 1 which shows the price of a European put option plotted against the volatility, $\sqrt{\sigma}$, and the asset price, S . The parameters used for this calculation are given in Table 1.

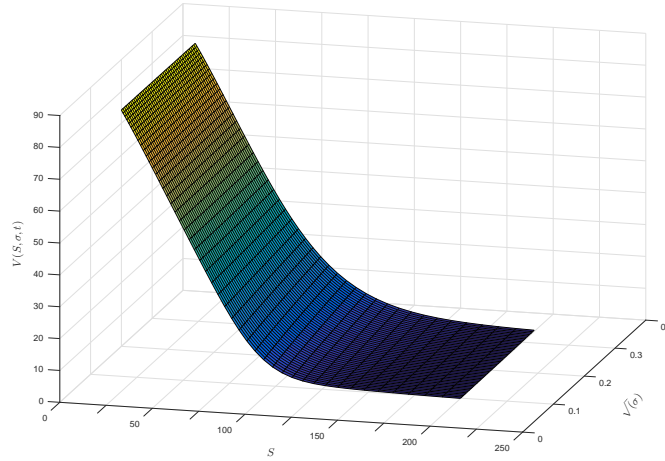


Figure 1: Price of a European Put Option

Parameter	Value
Strike Price	$K = 100$
Time to maturity	$T = 0.5$
Interest rate	$r = 0.05$
Volatility of volatility	$v = 0.1$
Mean reversion speed	$\kappa = 2$
Long-run mean of σ	$\theta = 0.01$
Correlation	$\rho = -0.5$
Jump Intensity	$\lambda = 0.2$

Table 1: Default parameters for numerical simulations.

6.1. Numerical Convergence

We perform a numerical study to evaluate the rate of convergence of the scheme. We refer to both the l_2 -norm error ϵ_2 and the l_∞ -norm error ϵ_∞ with respect to a numerical reference solution on a fine grid with $h_{\text{ref}} = 0.025$. With the parabolic mesh ratio k/h^2 fixed to a constant value we expect these errors to converge as $\epsilon = Ch^m$ for some m and C which represent constants. From this we generate a double-logarithmic plot ϵ against h

which should be asymptotic to a straight line with slope m , thereby giving a method for experimentally determining the order of the scheme.

For comparative purposes we perform the same numerical study using a standard second-order central difference scheme. The second-order scheme requires a Rannacher style start-up [25] which involves starting by four quarter fully implicit Euler steps to combat stability issues [16].

These numerical convergence results are included in Figure 2 for the l_2 -norm error ϵ_2 and Figure 3 for the l_∞ -norm error ϵ_∞ . The numerical convergence orders are estimated from the slope of a least squares fitted line. We observe that the numerical convergence order agree well with the theoretical order of the schemes, with the new high-order compact scheme achieving convergence rates close to four.

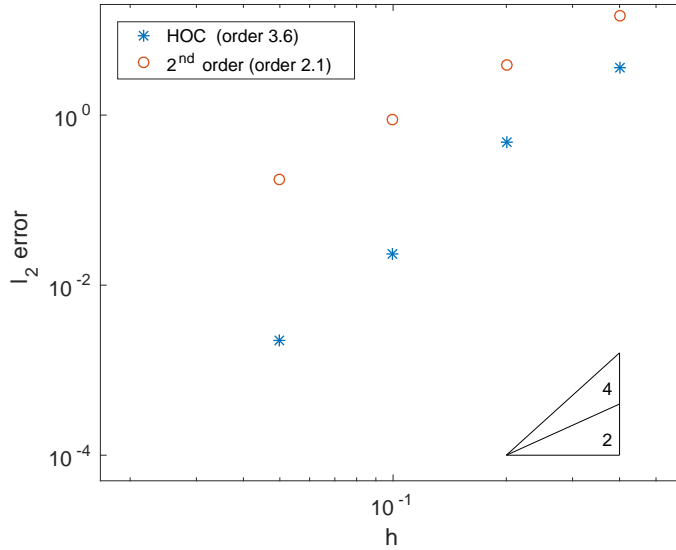


Figure 2: l_2 -error in option price taken at mesh-sizes, $h = (0.4, 0.2, 0.1, 0.05)$

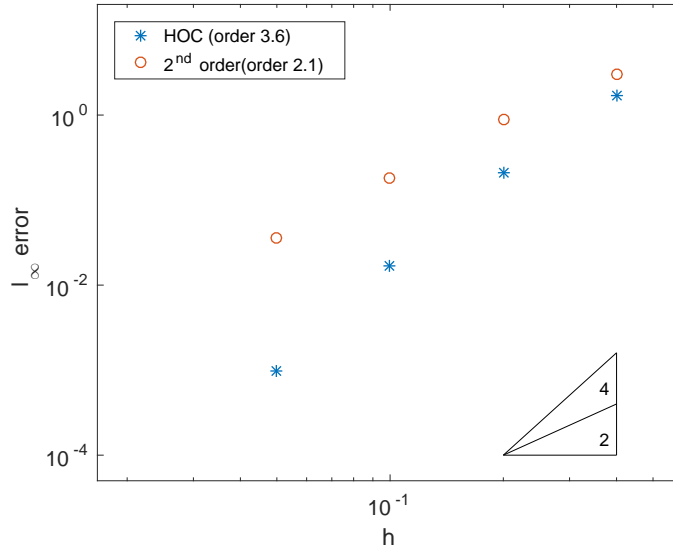


Figure 3: l_∞ -error in option price taken at mesh-sizes, $h = (0.4, 0.2, 0.1, 0.05)$

6.2. Numerical Stability Analysis

To assess the stability of the scheme we present a numerical stability analysis. We propose to test to what extent the parabolic mesh ratio k/h^2 impacts the convergence of the scheme. If the effect is minimal this will allow numerically regular solutions to be obtained without restriction on the time step-size. We proceed to compute numerical solutions for varying values of the parabolic mesh ratio k/h^2 and the mesh width h , then plot these against the associated l_2 -norm errors to detect stability restrictions depending on k/h^2 . This numerical test is performed for both the high-order and the second-order schemes, with the results shown in Figure 4 and Figure 5 respectively. We use default parameters from Table 1, and vary the parabolic mesh size from 0.1 to 1 in increments of 0.1. Note the difference in the error scales between the two schemes.

For both schemes the error increases gradually as the parabolic mesh ratio and h are increased. We note that for the second-order scheme the contour plot of the error may indicated some mild condition on the time stepping, the effect being stronger for larger mesh size h . The high-order scheme also features a mild dependence on the parabolic mesh ratio. Although there is no apparent stability restriction, it appears that values of the parabolic mesh ratio below and close to 0.5 are most useful. We attribute this dependence of the scheme to the parabolic mesh ratio as a consequence of the implicit-explicit nature of the scheme. For the present option pricing problem, the restriction on the time stepping for the new scheme is not severe, since the discretisation matrices do not change in time (the coefficients in the partial integro-differential equation (2) do not depend on time). Hence, the sparse matrix factorisation is performed only once, and additional time steps do not require additional factorisations to solve the problem.

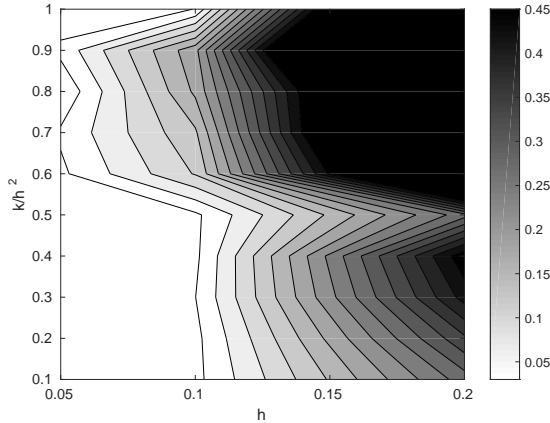


Figure 4: Contour plot of the l_2 -norm error for the HOC scheme.

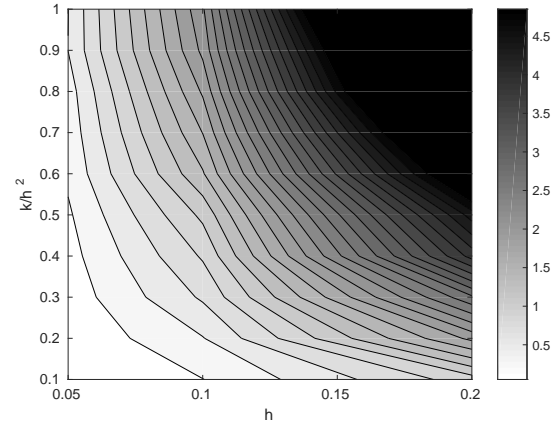


Figure 5: Contour plot of the l_2 -norm error for second-order scheme

6.3. Computational efficiency comparison

We conduct an efficiency comparison between the new high-order scheme and a standard second-order discretisation. We compare the computation time to obtain a given accuracy, taking into account matrix setups, factorisation and boundary condition evaluation. The timings depend obviously on technical details of the computer as well as on specifics of the implementation. Care was taken to implement both schemes in an efficient and consistent manner to avoid unnecessary bias in the results. All results were computed on the same laptop computer (2015 MacBook Air 11”).

Since the coefficients in (2) do not depend on time, we are required to build up the discretisation matrices for the new scheme only once (twice for the second-order scheme with Rannacher start-up). The new scheme requires only one initial LU -factorisation of a sparse matrix. This factorisation is then employed in each time step, leading to a highly efficient scheme. Further efficiency gains are obtainable by parallelisation or GPU computing.

The results are shown below in Figure 6. The mesh-sizes used for this comparison are $h = 0.4$, $h = 0.2$, $h = 0.1$ and $h = 0.05$, with the reference mesh-size used being $h = 0.025$. From this comparison it is clear to note that the high-order compact scheme achieves higher accuracy with less computation time at all mesh-sizes. The improvement in computation time can be partly attributed to the absence of the Rannacher start-up which requires the additional construction and factorisation of a sparse matrix populated with coefficients for the implicit Euler steps.

6.4. Hedging performance

The so-called Greeks (partial derivatives of the option price with respect to independent variables or parameters) are quantities which represent the market sensitivities of options. Delta measures the sensitivity of the option price with respect to the price the underlying

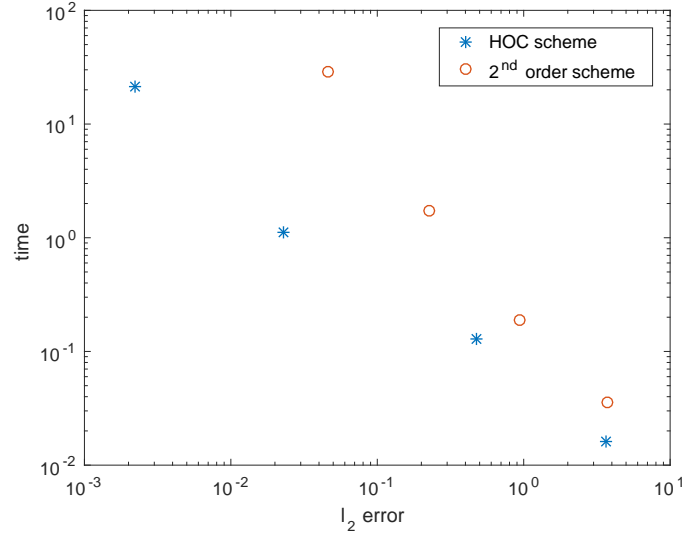


Figure 6: Computation speed comparison taken at mesh-sizes, $h = (0.4, 0.2, 0.1, 0.05)$

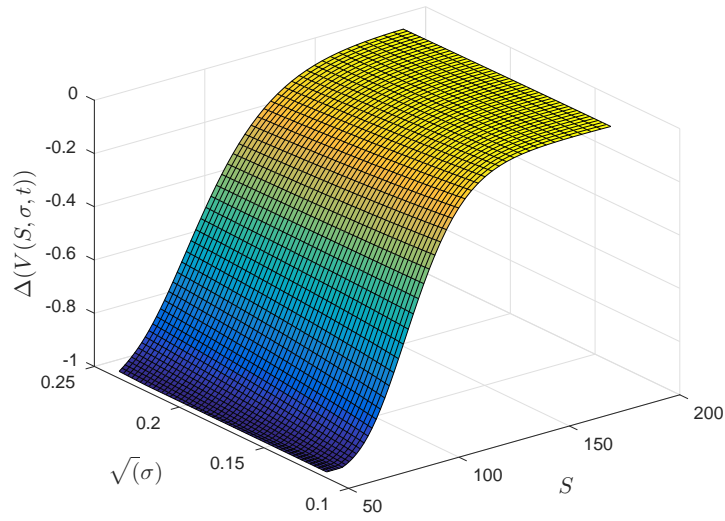


Figure 7: Delta of option $V(S, \sigma, t)$ with default parameters.

asset, i.e.

$$\Delta = \frac{\partial V}{\partial S}.$$

Delta Hedging is a common strategy employed by options traders, an options strategy that aims to hedge the risk associated with price movements in the underlying asset, by offsetting long and short positions. This strategy allows a trader to profit from potential shifts in volatility or the option duration, however to be fully hedged a trader must adapt their portfolio by managing the position in the underlying. In this instance the higher order convergence of our scheme may be of use to traders.

We propose that the higher-order convergence achieved in the option price will also be represented in the Delta of the option, and as a consequence we will achieve a better hedge.

We calculate the Delta from the option price $V(S, \sigma, t)$. To maintain the order of the scheme we use the following fourth-order approximation formula with the boundaries trimmed to remove the need for extrapolation,

$$\Delta_{i,j} = \frac{1}{S_j} \frac{u(i, j-2) - 8u(i, j-1) + 8u(i, j+1) - u(i, j+2)}{12h}.$$

Figure 7 shows the resulting Delta of a European put option. Through the same numerical convergence method used for the option price we examine the convergence of the Delta with respect to a numerical reference solution. The results are seen in Figures 8 and 9. We observe also here that the numerical convergence order agree well with the theoretical order of the schemes, with the new high-order compact scheme achieving convergence rates between three and four.

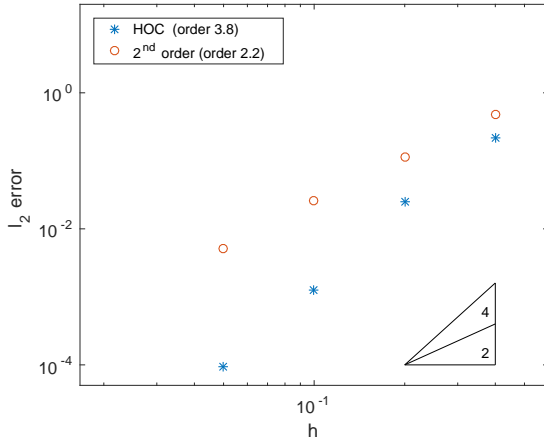


Figure 8: l_2 -error in Delta

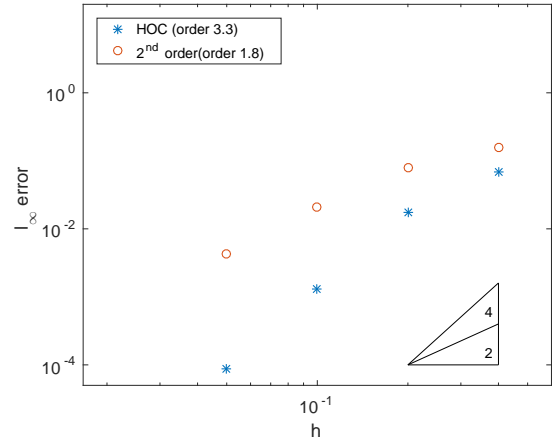


Figure 9: l_∞ -error in Delta

6.5. Delta Hedging - Delta Neutral Portfolio

We construct a Delta-neutral portfolio $\Pi = P - \Delta S$ to measure the accuracy of the hedge, the value of this portfolio should not be affected by any change in the underlying asset. We conduct the test on a fine reference grid with mesh-size, $h_{\text{ref}} = 0.025$ then we compare

the performance of each subsequent mesh-size. For comparative purposes this test is also conducted using the second-order scheme central difference scheme.

We now examine the percentage error introduced into the value of each portfolio in comparison to the reference grid. This test is conducted by moving the asset price up or down by a fixed amount. The results for this experiment are shown in Table 2 and Table 3, with the parameters shown in Table 1. We observe that our base case is satisfied and the high-order scheme offers a better delta hedge, even on a coarser grid.

Mesh Size	High-order	2nd order
$h = 0.4$	5.7649	10.3354
$h = 0.2$	0.3505	2.2765
$h = 0.1$	0.0083	0.5598
$h = 0.05$	$7.33 \cdot 10^{-4}$	0.1137

Table 2: Percentage error in portfolio value for a move down in the underlying.

Mesh Size	High-order	2nd order
$h = 0.4$	4.6914	6.4067
$h = 0.2$	0.2980	1.0895
$h = 0.1$	0.0074	0.2417
$h = 0.05$	$7.86 \cdot 10^{-4}$	0.0493

Table 3: Percentage error in portfolio value for a move up in the underlying.

7. Conclusions

We have derived a new high-order compact finite difference method for option pricing in stochastic volatility jump models. Numerical experiments confirm high-order convergence in both the option price and the delta of the option. The method is based on an implicit-explicit scheme in combination with high-order compact finite difference stencils for solving the partial integro-differential equation. It can be implemented in a highly efficient manner and can be used to upgrade existing finite difference codes. Examples of a delta hedged portfolio provide clear evidence that the high-order scheme is valuable for industry professionals seeking to calculate the relevant delta accurately and requiring fastest computational time.

A straightforward extension of this paper is the introduction of the SVCJ model which allows for jumps in both returns and volatility. As a second extension, one can combine the method presented in this paper with high-order alternating direction implicit methods as in [14, 17, 12]. We leave these extensions for future research.

Acknowledgement.

BD acknowledges partial support by the Leverhulme Trust research project grant ‘Novel

discretisations for higher-order nonlinear PDE' (RPG-2015-69). AP has been supported by a studentship under the EPSRC Doctoral Training Partnership (DTP) scheme (grant number EP/M506667/1).

References

- [1] D.S. Bates, Jumps and stochastic volatility: Exchange rate processes implicit Deutsche mark options, *Rev. Financ. Stud.* **9**, 637-654, 1996.
- [2] E. Benhamou, E. Gobet and M. Miri. Time Dependent Heston Model, *SIAM J. Finan. Math.* **1**, 289-325, 2010.
- [3] F. Black and M. Scholes. The pricing of options and corporate liabilities. *J. Polit. Econ.* **81**, 637-659, 1973.
- [4] M. Briani, R. Natalini and G. Russo, Implicit-explicit numerical schemes for the jump-diffusion processes, *Calcolo* **44**, 33-57, 2007.
- [5] N. Clarke and K. Parrott. Multigrid for American option pricing with stochastic volatility. *Appl. Math. Finance* **6**(3), 177-195, 1999.
- [6] R. Cont and P. Tankov, *Financial Modelling with Jump Processes*, Chapman & Hall/CRC, Boca Raton, FL, 2004.
- [7] D. Duffie, J. Pan and K. Singleton, Transform analysis and asset pricing for affine jump-diffusions, *Econometrica*, **68**(6), 1343-1376, 2000.
- [8] D. Duffie, Numerical Analysis of Jump Diffusion Models: A Partial Differential Equation Approach, Technical Report, Datasim, 2005.
- [9] B. Düring and M. Fournié, High-order compact finite difference scheme for option pricing in stochastic volatility models, *J. J. Comp. Appl. Math.* **236**, 4462-4473, 2012.
- [10] B. Düring, M. Fournié and C. Heuer, High-order compact finite difference scheme for option pricing in stochastic volatility models on non-uniform grids, *J. Comp. Appl. Math.* **271**, 247-266, 2014.
- [11] B. Düring, M. Fournié, and A. Rigal. High-order ADI schemes for convection-diffusion equations with mixed derivative terms. In: *Spectral and High Order Methods for Partial Differential Equations - ICOSAHOM'12*, M. Azaïez et al. (eds.), pp. 217–226, Lecture Notes in Computational Science and Engineering 95, Springer, Berlin, Heidelberg, 2013.
- [12] B. Düring, C. Hendricks and J. Miles, Sparse grid high-order ADI scheme for option pricing in stochastic volatility models. preprint, arXiv:1611.01379, 2016.

- [13] B. Düring and C. Heuer, High-order compact schemes for parabolic problems with mixed derivatives in multiple space dimensions, *SIAM J. Numer. Anal.* **53**(5), 2113-2134, 2015.
- [14] B. Düring and J. Miles. High-order ADI scheme for option pricing in stochastic volatility models. *J. Comput. Appl. Math.* **316**, 109-121, 2017.
- [15] M. Fakharany, R. Company and L. Jódar. Positive finite difference schemes for a partial integro-differential option pricing model. *Appl. Math. Comp.* **249**, 320-332, 2014.
- [16] M.B. Giles and R.J. Carter, Convergence analysis of Crank-Nicholson and Rannacher time-marching, *J. Comput. Financ.* **9**, 89-102, 2006
- [17] C. Hendricks, C. Heuer, M. Ehrhardt and M. Günther, High-order ADI finite difference schemes for parabolic equations in the combination technique with applications in finance, *J. Comput. Appl. Math.* **316**, 175-194, 2017.
- [18] S.L. Heston. A closed-form solution for options with stochastic volatility with applications to bond and currency options. *Rev. Financ. Stud.* **6**(2), 327-343, 1993.
- [19] K.J. in't Hout and S. Foulon. ADI finite difference schemes for option pricing in the Heston model with correlation. *Int. J. Numer. Anal. Mod.* **7**, 303-320, 2010.
- [20] N. Hilber, A. Matache and C. Schwab. Sparse wavelet methods for option pricing under stochastic volatility. *J. Comput. Financ.* **8**(4), 1-42, 2005.
- [21] S. Ikonen and J. Toivanen. Efficient numerical methods for pricing American options under stochastic volatility. *Numer. Methods Partial Differential Equations* **24**(1), 104-126, 2008.
- [22] H.O. Kreiss, V. Thomée and O. Widlund, Smoothing of initial Data and Rates of Convergence for Parabolic Difference Equations, *Comm. Pure Appl. Math.* **23**, 241-259, 1970.
- [23] A.L. Lewis. *Option valuation under stochastic volatility*. Finance Press, Newport Beach, CA, 2000.
- [24] R.C. Merton. Option pricing when underlying stock returns are discontinuous. *J. Financ. Econ.* **3**(1-2), 125-144, 1976.
- [25] R. Rannacher, Finite element solution of diffusion problems with irregular data, *Numer. Math.*, **43**, 309-327, 1984.
- [26] M.J. Ruijter and C.W. Oosterlee. Two-dimensional Fourier cosine series expansion method for pricing financial options, *SIAM J. Sci. Comp.* **34**(5), 642-671, 2012.
- [27] E.W. Sachs and A.K. Strauss, Efficient solution of a partial integro-differential equation in finance, *Appl. Numer. Math.* **58**, 1687-1703, 2008.

- [28] S. Salmi and J. Toivanen, An IMEX-scheme for pricing options under stochastic volatility with jumps, *Appl. Numer. Math.* **84**, 33-45, 2014.
- [29] S. Salmi, J. Toivanen and L. von Sydow, An IMEX-scheme for pricing options under stochastic volatility models with jumps, *SIAM J. Sci. Comp.*, **36**(5), B817-B834, 2014.
- [30] L. von Sydow, J. Toivanen and C. Zhang, Adaptive finite difference and IMEX time-stepping to price options under Bates Model, *Int. J. Comput. Math.*, **92**(12), 2515-2529, 2015.
- [31] D. Tavella and C. Randall. *Pricing Financial Instruments: The Finite Difference Method*. John Wiley & Sons, 2000.
- [32] W. Zhu and D.A. Kopriva. A spectral element approximation to price European options with one asset and stochastic volatility. *J. Sci. Comput.* **42**(3), 426–446, 2010.
- [33] R. Zvan, P.A. Forsyth and K.R. Vetzal. Penalty methods for American options with stochastic volatility. *J. Comp. Appl. Math.* **91**(2), 199–218, 1998.